M. Hermann, M.D. and P. Sloniewski, M.D.

New Proposed Magnetic Resonance Areas of the Cavernous Sinus and Their Relationship to the Neurosurgical Triangles

ABSTRACT—MRI appears to be the best contemporary method with which to evaluate cavernous sinus anatomy. Based on anatomic landmarks that are easily detectable in the standard MRI examination, the cavernous sinus is divided into six areas. Each of the newly defined areas corresponds to the previously described neuroanatomic triangles. Evaluation of the newly defined areas in a plane perpendicular to these triangles on a MRI scan permits expansion of these two-dimensional areas into three-dimensional spaces; thus, the neurosurgical approach can be observed and their anatomic and pathologic content examined. Radiologic and surgical evaluation of the cavernous sinus is presented.

The number of neurosurgical procedures performed within the cavernous sinus has been growing rapidly. Numerous anatomic descriptions and surgical approaches to the cavernous sinus have been introduced.[1–4] MRI is the best contemporary tool of presurgical evaluation of the cavernous sinus and its contents.[5–7]

The purpose of this article is to correlate the cavernous sinus anatomy and surgical approaches with their MRI counterpart. Based on anatomic landmarks that are easily detectable by standard MRI examination, which included the oculomotor nerve, cranial nerve II, Meckel's cave, petrosal bone, the foramen lacerum, and the anterior and posterior clinoid processes, the cavernous sinus is divided into six areas. Each newly defined area corresponds to the previously described neuroanatomic triangles.[1] In addition, this study presents the content of the defined areas and main MRI landmarks. Any area, when observed perpendicular to its surface, becomes a line (Fig. 1). In this way, evaluation of the newly defined areas in plane perpendicular to the triangles on MRI scan permits expansion of these two-dimensional areas into three-dimensional spaces. This permits observation of the potential neurosurgical approach and examination of its anatomic and pathologic content. The suggested MRI areas are larger than any previously described surgical triangle. A primary objective of the study was to group some anatomic triangles and systematize the MR anatomy of the part of the central skull base region. Consequently, we attempted to link radiologic and surgical evaluation of the cavernous sinus. The newly defined areas were divided into coronal and sagittal groups adequate to the MRI plane of their optimal visualization. Four coronal and two sagittal areas are presented.

MATERIALS AND METHODS

MRI examinations were made on a 0.5-tesla (T) Philips Gyroscan NT (Philips Medical Systems, Best, The Netherlands) with a standard head coil. The TSE T_2-

Skull Base Surgery, Volume 10, Number 3, 2000 Instituto Medico Da Radiologia Clinica, Porto, Portugal (MH) and Neurosurgery Department (PS), Medical University of Gdansk, Gdansk, Poland. Reprint requests: Dr. M. Hermann, Instituto Medico Da Radiologia Clinica, Augusta Rosa 142, 4000 Porto, Portugal. E-mail: m617283@netscape.net 1052–1453,p;2000,10,03,119,124,ftx,en;sbs00189x

A B

Figure 1. MRI newly defined area **(A)**, visualized in perpendicular plane **(B)**, permitting evaluation of the neurosurgical approach to the area (large arrow) and its anatomic content (small arrows).

weighted sequence was obtained with the following parameters: TR 4000, TE 250, TSE factor 48, NSA 2, FOV 140, slice thickness 0.8 mm, gap 0 mm in sagittal and coronal planes. The scan time was 9 minutes, 43 seconds.

RESULTS

Table 1 presents the MRI areas, their main contents, and their correspondence to anatomic triangles:

Area C I (coronal I): This MRI area is on the coronal scan line from the oculomotor nerve after its entrance to the cavernous sinus to the second cranial nerve. Area C I contains anteromedial triangle. The main landmark inside area C I is the anterior clinoid process.

Area C II (coronal II): This MRI area is on the coronal scan line from the oculomotor nerve running inside the cavernous sinus to the upper edge of Meckel's cave. Area C II contains paramedial and Parkinson triangles.

Area C III (coronal III): This MRI area is on the coronal scan lateral wall of Meckel's cave and on lower part of the lateral wall of the cavernous sinus starting from foramen ovale to the superior orbital fissure. Area C III contains lateral and anterolateral triangles.

Area C IV (coronal IV): This MRI area is on the coronal scan, with the superior edge of the petrosal bone starting from its apex to the internal carotid artery in the foramen lacerum. Area C IV contains Kawase's (posteromedial) and Glasscock's (posterolateral) triangles.

Area S I (sagittal I): This MRI area is on the sagittal scan, with the superior wall of the cavernous sinus from the anterior clinoid process to the posterior clinoid processes and the apex of the petrosal bone apex. The main landmark of the area is the oculomotor nerve entering the superior wall of the sinus. Area S I contains oculomotor and carotid triangles.

Area S II (sagittal II): This MRI area is on the sagittal scan, with the posterior wall of the cavernous sinus and the posterior edge of the petrosal bone starting from the posterior clinoid process to the internal acoustic canal. The area S II contains inferomedial and inferolateral triangles.

DISCUSSION

The primary objective of this study was to define new anatomic areas of the cavernous sinus and to link them to the anatomic triangles.[1] We decided to delineate new cavernous sinus sections on the basis of area land-

Table 1. MR Areas, Their Main Counterparts, and Correspondence to Anatomic Triangles

MRI Plane, MRI Area	*No. of Anatomical Triangles Included*	*MR Contents of Selected Area*	*Corresponding Anatomical Triangles*[1]
Coronal C I	1	Anterior clinoid process, anterior loop, distal horizontal part and first supracavernous segment of ICA	Anteromedial
Coronal C II	2	Horizontal part and medial loop of ICA, most of CS venous spaces	Superior, Parkinson
Coronal C III	2	Trigeminal ganglion, all three divisions of trigeminal nerve, part of bony floor of middle cranial fossa, lateral loop of ICA	Far lateral, anterolateral
Coronal C IV	2	ICA in carotid canal and in foramen lacerum, posterior loop of the ICA, part of petrosal bone	Kawase, Glasscock
Sagittal S I	2	Oculomotor nerve entrance to the CS, venous spaces, medial loop, first portion of the horizontal part and the clinoid segment of ICA	Oculomotor, Carotid
Sagittal S II	2	Trigeminal nerve entering Meckel's cave, posterior wall of petrosal bone, Meckel's cave, posterior venous spaces, medial loop of the ICA	Posteroinferior

CS, cavernous sinus; ICA, internal carotid artery; MRI, magnetic resonance image.

marks that are easy detectable by standard MRI examination of the central scull base and that are key surgical landmarks.[8–11] Although the proposed markers can be observed on both standard T_1- and T_2-weighted images,[12] we used a heavily T_2-weighted thinly sliced sequence to obtain optimal delineation of the cavernous sinus anatomy. Our landmarks included the optic, oculomotor, and trigeminal nerves; Meckel's cave; petrosal bone; anterior and posterior clinoid processes; and the superior and posterior walls of the cavernous sinus.

The optic and the oculomotor nerves define the borders of the virtual triangular-shaped coronal C I area.[1] These linear structures on coronal MRI are seen as low intensity both in T_1 and T_2-wieghted sequences points (Fig. 2). Area C I can be readily detected because it is located below the anterior clinoid process that remains the low signal intensity on both T_1- and T_2-weighted MRI. The MRI of area C I corresponds to the surgical anatomy, as entry to the anteromedial triangle requires removal of the anterior clinoid process. On coronal MRI scans inside area C I, we can observe not only the anterior loop and the distal horizontal part of the internal carotid artery (Fig. 3) but also the first supracavernous segment of the artery. The fibrous rings surrounding the internal carotid artery and the ophthalmic artery cannot be observed on the coronal T_2-weighted images, probably owing to their small diameter.

Area C II is located within the part of the lateral wall of the cavernous sinus. Its borders are circumscribed by an oculomotor nerve and by the upper edge of the Meckel's cave and the ophthalmic division of the trigeminal nerve (Fig. 4). The chief structures inside the area are the horizontal part and medial loop of the internal carotid artery, a low-intensity structure in T_1- and T_2-weighted images. Most high signal intensity venous spaces of the cavernous sinus are also found within the above-mentioned area. One should be aware of the trochlear and abducens nerves inside this C II area but,

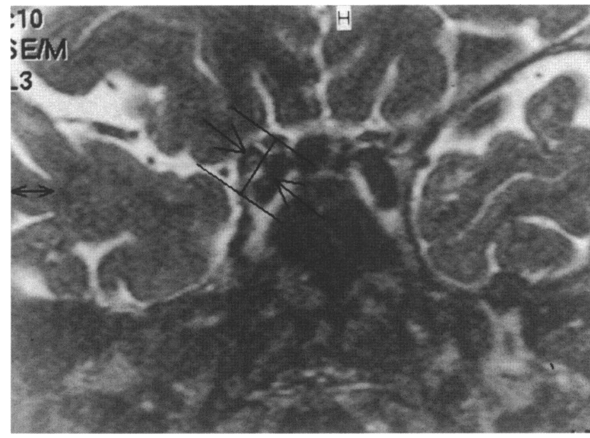

Figure 3. MRI area Coronal I (C I) contents, showing the anterior clinoid process (upper arrow) and the anterior loop of the internal carotid artery (lower arrow), both of low-intensity signal.

because of their small diameter, they are not always easily detectable on coronal MRI scans. Area C II encloses the Parkinson's and paramedial triangles.

Area C III consists of the lower section of the lateral wall of the cavernous sinus. Its borders are the ophthalmic division of the trigeminal nerve through the lateral wall of Meckel's cave to the lower edge of the cave. Through the area C III trigeminal ganglion, all three divisions of the trigeminal nerve and part of the bony floor of the middle cranial fossa can be observed on MRI (Fig. 5). Little venous spaces with a high-intensity signal pattern surrounding the nerves in area C III can also be noticed. Lying inferomedially to the nerves in Meckel's cave, the lateral loop of the internal carotid artery can be easily inspected (Fig. 6). Area C III contains the anterolateral and lateral surgical triangles.

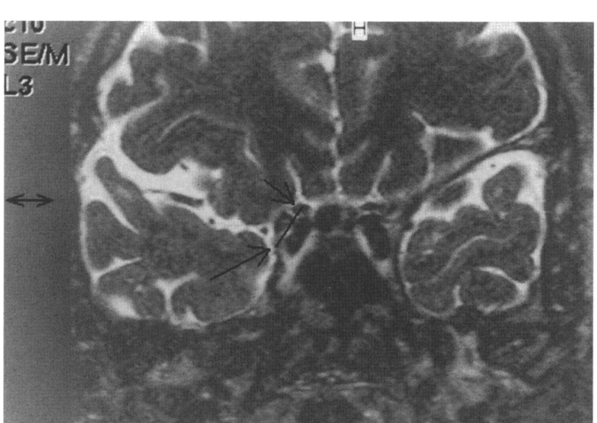

Figure 2. MRI area Coronal I (C I) (line) between the optic nerve (short arrow) and the oculomotor nerve (long arrow).

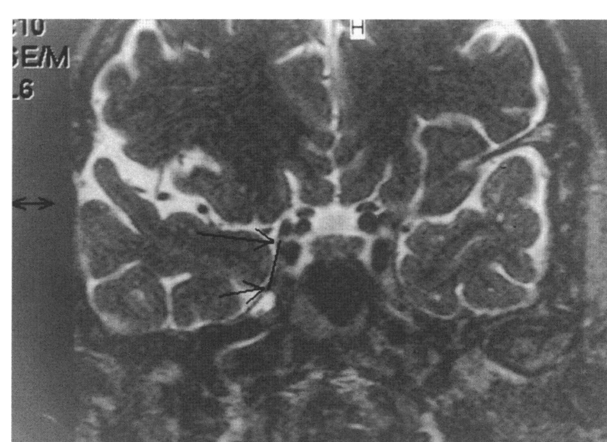

Figure 4. MRI Coronal II (C II) area (line) between the oculomotor nerve (long arrow) and the superior edge of Meckel's cave (short arrow).

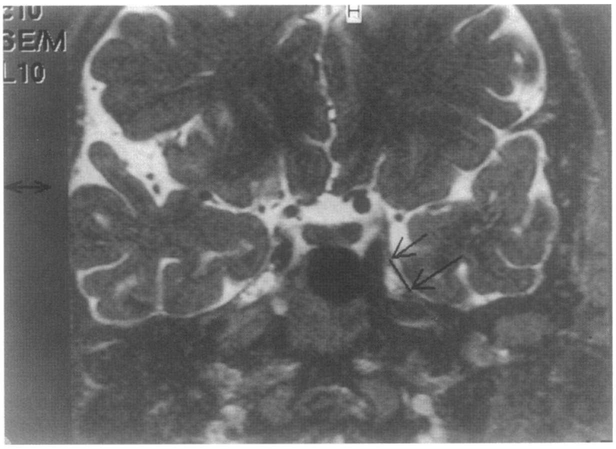

Figure 5. MRI area Coronal III (C III) (line) between the superior (short arrow) and the inferior edge (long arrow) of Meckel's cave.

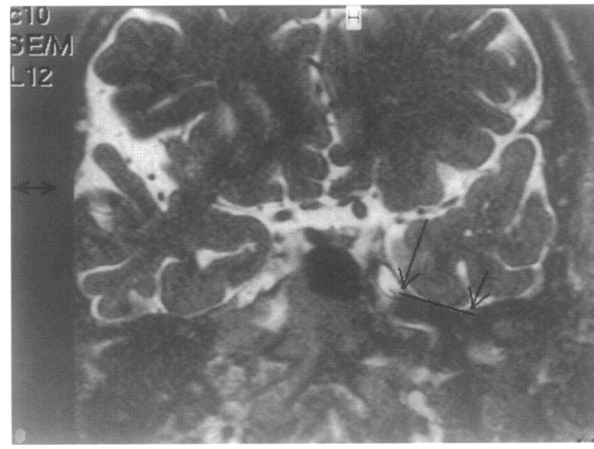

Figure 7. MRI area Coronal IV (C IV) (line) from the apex of petrosal bone (long arrow) to the foramen lacerum (short arrow).

Area C IV consists of the superior edge of the petrosal bone starting from its apex to the internal carotid artery in the foramen lacerum. In this area, the main landmark is the internal carotid artery in the carotid canal running forward to the foramen lacerum with its posterior loop (Fig. 7). The bony structure of the petrosal bone can also be observed. Area C IV contains posteromedial and posterolateral triangles.

On the sagittal images, two MRI areas can be distinguished. Sagittal S I area corresponds to superior wall of the cavernous sinus. On the T_2-weighted images the superior wall is a linear low-intensity structure and is surrounded from the above by high signal intensity subarachnoid space and from below by high signal intensity venous spaces of the cavernous sinus. The markers of the area S I are the anterior and posterior clinoid processes, as well as the apex of the petrosal bone (Fig. 8). The oculomotor nerve entrance to the cavernous sinus through its dural foramen constitutes the key MRI landmark of this area. Segments of the internal carotid artery visible in MRI within area S I are the medial loop, the first portion of the horizontal part, and the clinoid segment of the artery (Fig. 9). The distal ring[1] of the artery is invariably seen on sagittal images, as it fuses with the superficial layer of the dura. The proximal ring can be observed only occasionally (Fig. 9). The other MRI anatomic structures of the cavernous sinus within this area include the venous spaces and the proximal segment of the abducens nerve in the sinus. Area S I includes the neurosurgical oculomotor and carotid triangles.

Area S II extends from the posterior clinoid process to the inner auditory canal and it comprises the posterior

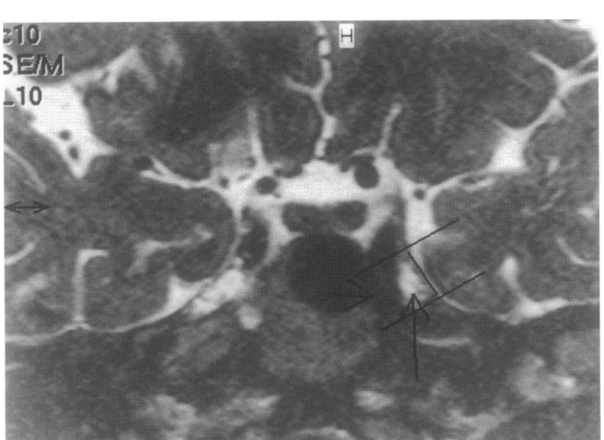

Figure 6. Within area Coronal III (C III) high-intensity signal of Meckel's cave (long arrow) and low-intensity signal of the lateral loop of the internal carotid artery (short arrow) can be observed.

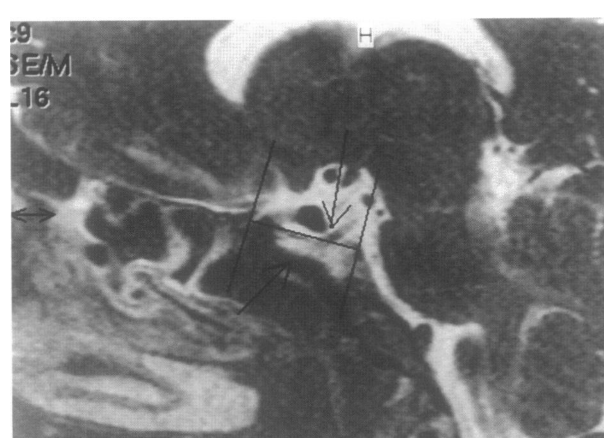

Figure 8. MRI area Sagittal I (S I) (nearly horizontal line) from the anterior to the posterior clinoid process. Note low signal intensity internal carotid artery and the oculomotor nerve entering the cavernous sinus.

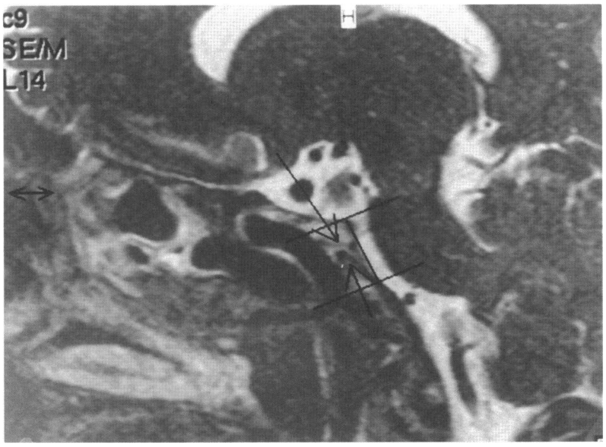

Figure 9. MRI area Sagittal II (S II) (nearly vertical line) from the posterior clinoid process to the inner auditory canal and its capacity, showing posterior venous spaces of the cavernous sinus (short arrow) and the abducens nerve in the sinus posterior to the internal carotid artery (long arrow).

wall of the cavernous sinus and the part of the posteromedial surface of the petrosal bone. The key MRI landmark of area S II is the trigeminal nerve entering Meckel's cave. Within this area on MRI scans, one can observe the posterior wall of the petrosal bone, Meckel's cave, the posterior venous spaces of the cavernous sinus, and, more anteriorly, the medial loop of the internal carotid artery (Fig. 9). The abducens nerve in Dorello's canal can be clearly visualized only on parasagittal images.

CASE REPORT

A 51-year-old woman presented with severe headache. MRI showed a pathological mass in the left cavernous sinus. MR angiography confirmed the aneurysm of the internal carotid artery. To examine the precise location of the aneurysm in the cavernous sinus, the MR areas on coronal scans were used. Optic nerve and oculomotor nerve entering the cavernous sinus, as well as the superior edge of the Meckel's cave were easily recognized on the coronal pre-contrast T_1-weighted images (Fig. 10). The aneurysm was found to be located within the coronal C II area between the oculomotor nerve and the first division of the trigeminal nerve so probably medial loop or the proximal horizontal segment of the internal carotid artery was the origin of the aneurysm. Area C II corresponds to the Parkinson's and paramedial neurosurgical triangles.

Figure 10. High-intensity signal aneurysm (asterisk) located in area Coronal II (C II) (line) between the oculomotor nerve (long arrow) and the superior edge of Meckel's cave (short arrow).

CONCLUSIONS

Coronal and sagittal MRI sequences are presumably the best present-day methods to evaluate main cavernous sinus landmarks and to define MRI areas. Direct interconnection of the new defined areas to the surgical triangles should be helpful in defining the pathologic borders within the cavernous sinus during MRI examination. It may be beneficial in finding the neck of the aneurysm in the sinus as well, which contribute to planning the optimal operational strategy.

REFERENCES

1. Dolenc V. Anatomy and Surgery of the Cavernous Sinus. New York: Springer-Verlag, 1989
2. Kawase T, van Loveren H, Keller JT, Tew JM. Meningeal architecture of the cavernous sinus: clinical and surgical implications. Neurosurgery 1996;39:527–534, 534–536
3. Oikawa S, Kyoshima K, Kobayashi S. Surgical anatomy of the juxta-dural ring area. J Neurosurg 1998;89:250–254
4. Seoane E, Rhoton A, de Oliveira E. Microsurgical anatomy of the dural collar (carotid collar) and rings around the clinoid segment of the internal carotid artery. Neurosurgery 1998;42: 869–886
5. Guy RL, Benn JJ, Ayers AB, Bingham JB, Lowy C, Cox TC, Sonksen PH. A comparison of CT and MRI in the assessment of the pituitary and parasellar region. Clin Radiol 1991;43: 156–161
6. Demaerel P, Marchal G, Casteels I, et al. Intracavernous aneurysm. Superior demonstration by magnetic resonance angiography. Neuroradiology 1990;32:322–324
7. Bradac GB, Riva A, Schorner W, Stura G. Cavernous sinus meningiomas: An MRI study. Neuroradiology 1987;29:578–581
8. Kobayashi S, Goel A, Hongo K. Neurosurgery of Complex Tumors and Vascular Lesions. Edinburgh: Churchill Livingstone, 1995
9. Apuzzo M. Brain surgery: Complication avoidance and management. Vol II. Edinburgh: Churchill Livingstone, 1993
10. Sekhar LN, Janecka IP. Atlas of skull base surgery. Philadelphia: Lippincott-Raven, 1993
11. Torrens M, Al-Mefty O, Kobayashi S. Operative Skull Base Surgery. New York: Churchill Livingstone, 1997
12. Daniels DL, Pech P, Mark L, Pojunas K, Williams AL, Haughton VM. Magnetic resonance imaging of the cavernous sinus. AJR 1985;144:1009–1014